FULL PAPER

PPS www.rsc.org/pps

Water splitting with silver chloride photoanodes and amorphous silicon solar cells

Antonio Currao,*[a] Vanga Raja Reddy,[a] Marieke K. van Veen,[a] Ruud E. I. Schropp[b] and Gion Calzaferri[a]

[a] *University of Bern, Department of Chemistry and Biochemistry, Freiestrasse 3, Bern, Switzerland 3012. E-mail: currao@iac.unibe.ch*

[b] *Utrecht University, Debye Institute, SID–Physics of Devices, 3508 TA Utrecht, The Netherlands P. O. Box 80000*

Received 2nd August 2004, Accepted 2nd September 2004
First published as an Advance Article on the web 24th September 2004

A thin silver chloride layer deposited on a conducting support photocatalyzes the oxidation of water to O_2 in the presence of a small excess of silver ions in solution. The light sensitivity in the visible part of the spectrum is due to self-sensitization caused by reduced silver species. Anodic polarization reoxidizes the reduced silver species. To test its water splitting capability, AgCl photoanodes as well as gold colloid modified AgCl photoanodes were combined with an amorphous silicon solar cell. The AgCl layer was employed in the anodic part of a setup for photoelectrochemical water splitting consisting of two separate compartments connected through a salt bridge. A platinum electrode and an amorphous silicon solar cell were used in the cathodic part. Illumination of the AgCl photoanode and the amorphous Si solar cell led to photoelectrochemical water splitting to O_2 and H_2. For AgCl photoanodes modified with gold colloids an increased photocurrent, and consequently a higher O_2 and H_2 production, were observed.

Introduction

To halt the buildup of greenhouse gases many nations are committed to decrease their production by supporting their own regional or national programs, agreeing to fulfill international short-term (Kyoto protocol),[1] or increasingly support long-term (C&C, contraction and convergence)[2] measures to mitigate climate change. Nevertheless, the development of an alternate energy source to fossil fuels becomes more and more important for getting under control the global atmospheric concentration of CO_2, the main greenhouse gas. H_2 has the potential to meet the requirements as a clean non-fossil fuel in the future, if it can be produced using the world's most abundant energy source, the sun, and safely stored and transported.[3]

The sun is our primary source of energy and compared to our life expectancy an inexhaustible resource. Solar energy has successfully been stored chemically by nature through photosynthesis.[4] The photochemical reaction which occurs in the photosynthetic process is the oxidation of water to O_2 by photosystem II and the reduction of $NADP^+$ to NADPH by photosystem I ($H_2O + NADP^+ +$ *solar energy (photons)* $\rightarrow \frac{1}{2}O_2 + 2H^+ + NADPH$). In the dark reaction of photosynthesis, NADPH is used together with ATP and water to reduce CO_2 to form carbohydrates. In effect then, water is split into O_2 and H_2, where the hydrogen is not in the gaseous form but bound by carbon. The aim of *artificial photosynthesis* is the solar splitting of water in O_2 and H_2, driven by a non-biological system. For that purpose, materials are necessary which upon light absorption can drive the water splitting reaction. Different ways have been chosen to convert solar energy into a chemically stored form as H_2.[3,5] Photoelectrolysis is the general term used to describe light-driven water splitting based on semiconductors. There are a number of approaches possible.[6] Basically, arrangements using either photovoltaic cells or semiconductor–liquid junctions, or combinations of the two were realized.

One approach based on solid-state photovoltaics is to couple a photovoltaic system and the electrolyser into a single system. An early report described the use of multiple junction semiconductor structures for the conversion of light energy to chemical energy when immersed in an electrolyte and exposed to light.[7] Semiconductor layers with different band gaps are connected in series, one behind the other, in a single monolithic device capable of generating the potential needed to split water. These so-called tandem cells are modified with or connected to H_2 and O_2 producing electrodes, like Pt and RuO_2-modified Pt, which act as cathode and anode, respectively.[8] For example n–p $GaInP_2/GaAs$,[9,10] n–p $Al_xGa_{1-x}As/Si$,[11] and multiple junction p–i–n amorphous Si[10,12] tandem cells were used for the photoelectrolysis of water.

Recently, another approach based on solid-state photovoltaics and solar driven water electrolysis at elevated temperatures was reported.[13] The basis behind this is the decrease of the electrochemical water splitting potential with increasing temperature. Solar radiation is used for generating the necessary potential by illuminating photovoltaic cells as well as for the heat source to facilitate water electrolysis. This permits smaller band gap solar cells to drive the water cleavage at sufficiently low temperatures (500 °C) from molten NaOH.

For arrangements based on semiconductor–liquid junctions, the water splitting potential is generated directly at the semiconductor–liquid interface. The ability of a semiconductor photoelectrode to drive the water splitting reaction is determined by its band gap and the position of the valence and conduction band edges relative to the water redox reactions. Semiconductor materials have been used to drive the water oxidation and reduction at the same time. Undoped[14] or Ni-doped $InTaO_4$,[15] $InNbO_4$,[14] $Ln_2Ti_2O_7$ (Ln = La, Pr, Nd),[16] $MCo_{1/3}Nb_{2/3}O_3$ (M = Ca, Sr, Ba),[17] $RbNdTa_2O_7$,[18] $NaTaO_3$ doped with La,[19] La_3TaO_7 or La_3NbO_7,[20] are examples where photocatalytic water splitting under light irradiation was described. For all these materials, the photocatalytic activity increases significantly when loaded with a reducing and/or oxidizing co-catalyst, such as Pt, RuO_2 or NiO. More promising is a photoelectrolysis cell based on two illuminated semiconductor–liquid junctions, an n-type for the evolution of O_2 and a p-type for the evolution of H_2. By separating the oxidation and reduction processes into half cell reactions, one can deal with one reaction at a time. Besides, two

DOI: 10.1039/b411882k

semiconductors with smaller band gaps can be utilized since each needs only to provide part of the water splitting potential. The smaller band gap means more absorption in the visible region of the solar spectrum where the sun has a greater photon flux. As a result, the maximum theoretical efficiency is considerably higher.[5,21] Proper selection of both semiconductor electrode characteristics ensures that the energy necessary for water photoelectrolysis is gathered entirely from the illumination, eliminating the necessity of applying energy from an external source. The same semiconductor material with just different doping was used to split water without any external bias. Single crystals of N-doped n-SiC and Al-doped p-SiC were employed as photoelectrodes in a photoelectrochemical cell.[22] Powders of two different semiconductor photocatalysts were also used for water splitting in the presence of a redox mediator. For the O_2 and H_2 evolution Pt-loaded WO_3 and Pt-loaded $SrTiO_3$ (doped with Cr, Ta), respectively, were used in an aqueous solution with the IO^-_3/I^- redox pair as mediator.[23] Polycrystalline n-Fe_2O_3 photoanodes have been investigated in a photoelectrochemical cell where the cathode was Zn-doped p-GaP[24] or p-Cu_2O.[25] Spontaneous water splitting under visible light illumination was reported, though the efficiency of the process remained low. In the latter experiment the photoelectrolysis cell had a separate compartment for the Fe_2O_3 anode and the cathode. The anode compartment had an alkaline electrolyte, whereas for the cathode compartment an acidic electrolyte was used. Consequently, the thermodynamic (theoretical) voltage needed to split water was considerably reduced due to the pH gradient present between the compartments (chemical bias).

A combination of the previously mentioned approaches leads to a setup where a photovoltaic cell is used together with a semiconductor that is in direct electrolyte contact. In this case the photovoltaic cell can be either combined with a reduction or with an oxidation photocatalyst. The water splitting reaction involves a two-electron reducing process for the H_2 production and a four-electron oxidizing process for the O_2 producing part. It is the water oxidation reaction that poses the greatest difficulty in achieving photocatalytic water splitting, mainly because accumulating four oxidative equivalents is required. Interestingly, reports of semiconductors focusing only on the photocatalytic H_2 production are scarcely found in the literature. For example, $CuMnO_2$[26] or platinized CdS[27] particle suspensions, or $LaMnO_3$/CdS nanocomposites[28] were reported to evolve H_2 without any external bias in the presence of hole scavengers under illumination. Transition metal loaded WS_2 showed photocatalytic H_2 production in the presence of a photosensitizer, an electron relay, and a sacrificial agent.[29] Sacrificial agents were also used in separate water reduction and oxidation experiments with the same oxide semiconductor. For $Ln_2Ti_2S_2O_5$ (Ln = lanthanide)[30] and $MCrO_4$ (M = Sr, Ba)[31] H_2 production was reported in the presence of sacrificial electron donors or O_2 production when sacrificial electron acceptors were present in solution.

Research work focusing on the oxidation of water to O_2 is also carried out by different research groups. A non-semiconductor based approach is to mimic the O_2 evolving center of photosystem II in photosynthesis.[32] Manganese complexes have been studied as models for artificial water oxidation to O_2.[33] For the semiconductor-based photoelectrolysis, different compounds have been explored as oxidation catalysts. Increased photochemical water oxidation was observed when ruthenium complexes used as sensitizers were adsorbed on RuO_2 in the presence of a sacrificial electron acceptor.[34] Carbon-[35] or nitrogen-doped TiO_2,[36] undoped[37] or Mg-doped WO_3,[38] Ta-,[25] Ti-, or Al-doped Fe_2O_3,[39] and $BiVO_4$[40] are all semiconductors able to split water when an external potential is applied. As mentioned above, the bias might be provided by a photovoltaic cell leading to a device for the photoelectrolysis of water. Tungsten trioxide (WO_3) or iron oxide (Fe_2O_3) photoanodes were connected in-series with a nanocrystalline dye-sensitized TiO_2 solar cell.[41] The short wavelength portion of the solar spectrum is absorbed by the photoanode. A nanocrystalline dye-sensitized TiO_2 solar cell is placed behind the transparent photoanode, capturing the long wavelength portion of the solar spectrum. The photovoltage generated by the second photosystem enables the generation of H_2 at a platinum cathode.

In this work, we present a different approach towards water photoelectrolysis where a semiconductor photoanode is used together with a photovoltaic cell. An AgCl photoanode was combined with a single junction amorphous silicon solar cell connected to a platinum cathode. The AgCl layer was employed in the anodic part and the platinum electrode in the cathodic part of a setup for water photoelectrolysis consisting of two separate compartments connected through a salt bridge. Illumination of both the AgCl photoanode and the amorphous Si solar cell led to photoelectrochemical water splitting to O_2 and H_2. A schematic representation of the principle is shown in Fig. 1. On one side, the photoanode oxidizes water to O_2, and on the other side the photocathode reduces water to H_2. The electron transfer from system 1 (photoanode) to system 2 (photocathode) is achieved by illumination. We also present the effect of gold colloids on the photocatalytic properties of AgCl photoanodes in photoelectrochemical water splitting experiments. An increased photocurrent, and consequently a higher O_2 and H_2 production were observed.

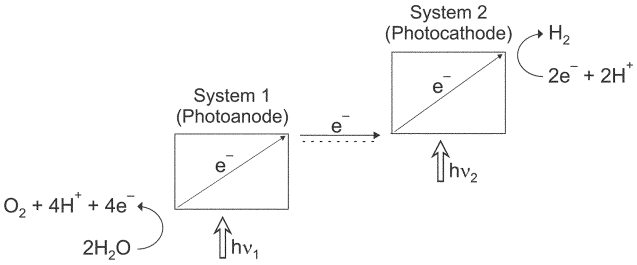

Fig. 1 Schematic representation of the photoelectrochemical water splitting experiment. For the oxidation of water to O_2 an AgCl photoanode was used (System 1). As the photocathode, a single junction amorphous silicon solar cell connected to a platinum cathode was employed for the H_2 production (System 2).

Experimental

Preparation of AgCl photoanodes

As glass support disks with a diameter of 24.5 mm and a thickness of 2 mm were used. The surface of the support was roughed by sandblasting. Two small grooves at the edge were used for mounting the support on the sample holder with poly(ethylene terephthalate) (PET) screws. A 50 nm thick Au layer was deposited as a conducting layer on the whole support. Next, a 150 nm Ag layer was deposited on almost the whole support, except for a 1.5 mm wide rim at the edge of the grooves which were covered by pins. The Au rims were necessary for contacting the support to the holding device. Depositions of gold and silver layers were carried out by physical vapor deposition (PVD) in a high vacuum coating system (Bal-Tec, MED 020). The AgCl layers were prepared by electrochemical oxidation of the silver layer in 0.2 M KCl (Merck) aqueous solution at pH $\approx$ 2, adjusted with 25% HCl (Hänseler AG). A three-electrode setup was used, where the coated glass support was the working electrode, a platinum wire was the counter electrode, and an Ag/AgCl electrode was the reference electrode (0.222 V *vs.* NHE, normal hydrogen electrode). With a computer-controlled potentiostat (EG&G, model 273A), an anodic potential sweep from 0.0 to 0.9 V was performed at a rate of 100 mV s^{-1}. After oxidation of the Ag layers, the color of the electrochemically produced AgCl electrodes was light-gray to gray indicating the presence of a small amount of reduced silver.

For Au colloid modified AgCl photoanodes, gold colloids were synthesized by the Turkevich method by simple reduction of gold chloride with sodium citrate.[42] 1 mL of a 5 mM tetrachloroauric(III) acid solution ($HAuCl_4 \cdot 3H_2O$, Merck) was transferred in a flask and diluted by adding 18 mL of water. The solution was heated until it began to boil. Then 1 mL of a 0.5% (17 mM) tri-sodium citrate solution ($C_6H_5Na_3O_7 \cdot 2H_2O$, Fluka) was added while stirring rapidly. The heating was continued until the color changed to pale purple. The flask was then removed from the heating element and stirring was continued until the solution cooled to room temperature. The solution was toped with water up to 20 mL to account for boiling losses. The gold particles produced are spherical in shape with a diameter of 15–20 nm. The final color of the colloidal gold solution was deep 'wine-like' red. Absorption spectra were recorded with a Lambda 900 spectrometer (PerkinElmer). The colloidal gold nanoparticles in solution have a broad absorption range with a maximum around 530 nm. The Au colloids were sedimented by immersing the AgCl layer into 5 mL of gold colloidal solution overnight. The next day, the layer was allowed to dry at room temperature.

The morphology of AgCl layers was investigated by scanning electron microscopy (SEM) conducted using a Hitachi S-3000N instrument operating at 20 kV. All AgCl electrodes are on glass supports. Electric contact of the AgCl layer with the sample holder was achieved by means of metal clips. The layers were not sputtered with gold.

Amorphous silicon solar cells

Hot-wire chemical vapor deposition (HWCVD) was used for the deposition of hydrogenated amorphous silicon films (a-Si:H) as the absorbing intrinsic layer in single junction n–i–p structured solar cells (n–i–p a-Si:H). The n- and p-doped layers were deposited by plasma enhanced chemical vapor deposition (PECVD). The layer thicknesses for the n, i, and p layers were ≈50 nm, ≈400–500 nm, and ≈20 nm, respectively. Unpolished stainless steel was used as the conducting support (≈0.1 mm). Indium-tin-oxide (ITO, In_2O_3:SnO_2) was deposited on top of the p layer using a mask, creating a pattern of square-shaped transparent ITO windows with an edge of 4 mm and a thickness of ≈80 nm each. The resistivity of the top transparent conductive oxide was lowered by the use of gold metal grid contacts on top of the ITO layer.[43] The cell matrix can easily be cut with scissors into smaller pieces. A wire was soldered onto the stainless steel support as back contact. For the front contact a pointed probe contact with a spherically shaped probe head was used. Only the area of a single solar cell, 16 mm^2, was illuminated during an experiment. The edges of the cell were covered with black insulating tape.

Experimental setup

Photoelectrochemical experiments were carried out in an apparatus consisting of two separate compartments connected through a salt bridge. One compartment was used for the AgCl photoanode, and the other for the cathode. A 50 nm Pt layer deposited by PVD on a conducting SnO_2:F-coated glass support (Siemens AG), as well as a Pt foil (0.1 mm thick, Johnson Matthey) were used as cathode. The apparatus was made of acrylic plastic (PMMA, poly(methyl methacrylate)). Both cell compartments had their own water and air tight inlets for the pH glass electrode, argon gas (inlet and outlet), pH control dispensing unit, and O_2 or H_2 sensor, respectively. Detection of O_2 and H_2 were carried out in situ by electrochemical measurement with sensors (WTW, model EO 96). For the calibration of the O_2 and H_2 sensors the anodic current signal, *i.e.*, the charge transferred from the photoanode to the cathode cell, was used to calculate conversion factors to scale the sensor signals accordingly (see ref. 46 for more details). A holding device was used for mounting and contacting the electrode in each cell. For the salt bridge a jelly-like electrolyte was used. A hot solution of 1.7 g of Agar (Fluka) in 100 ml 0.1 M KNO_3 (Merck) aqueous solution was poured into the bridge and left to solidify by cooling overnight. The electrolyte volume in both cells was approximately 75 ml. The anode and cathode compartments were filled with aqueous 0.1 M KNO_3, which was 1 mM in $AgNO_3$, and 0.1 M HNO_3 (Hänseler AG), respectively. Each cell compartment was magnetically stirred. In both cell compartments the pH was measured with a combination pH glass electrode (Thermo Orion, Ross pH electrode, internal filling solution: 1 M KNO_3), and maintained at 4.5 ± 0.5 for the photoanode and at ≈1 for the cathode cell. One dispensing unit for each cell compartment was used for adjusting the pH, if necessary, with 0.1 M KOH (Merck) or 0.1 M HNO_3 solution, respectively. The experiments were carried out at room temperature (≈23°C). Before data acquisition began, the electrolyte was thoroughly purged with argon. Both cell compartments were under argon atmosphere throughout all experiments. A 1000 W Xenon arc lamp was used as the light source (Osram, XBO 1000 W/HS OFR), with a power supply (LPS 1000) and lamp housing (A5000) from PTI. To reject the IR part of the lamp radiation, a stainless steel IR filter filled with distilled water as absorption liquid was placed on top of the lamp housing. The light beam was collimated with lenses and passed through a light filter (Schott, KG3; 50% transmission range: 330–700 nm), before it was split with a beam splitter (polka dot beam splitter, Oriel Instruments), illuminating the AgCl photoanode cell and the a-Si:H solar cell simultaneously. The incident light intensity at the location of the AgCl electrode and the a-Si:H solar cell was about 100 mW cm^{-2}, measured with a radiant power/energy meter (Oriel Instruments, model 70260). Due to the holding device and the electrolyte filling level, the illuminated area of the AgCl photoanode was around 2.5 cm^2. In all experiments, the AgCl photoanode and the a-Si:H solar cell cell were exposed to successive illumination and dark periods of 120 and 45 min duration each, respectively. During the dark periods of an experiment, the O_2 and H_2 sensor signals decreased in all results presented, because the setup was under constant inert gas purging. The front contact of the a-Si:H solar cell was connected to the AgCl photoanode, the back contact to the Pt cathode. The current flow during the experiment was monitored by measuring the voltage over a 10 ohm resistance. All the various components of the experimental setup were connected to a multimeter (Keithley, model 2000 with scanner card) that was controlled by a computer *via* a GPIB bus. Data acquisition was monitored and stored on file by a program written in QBasic. All presented results were smoothed and background corrected because of noise in the data recorded.

Results and discussion

Reaction mechanism

We have reported that appropriately prepared silver chloride electrodes photocatalytically oxidize water to O_2 under suitable conditions.[44–46] The nanostructured silver chloride layer acts as photocatalyst in the presence of a small excess of silver ions in solution, with a maximum evolution rate between pH 4 and 6. AgCl is a semiconducting material with an indirect band gap of 3.3 eV (≈380 nm).[47] The sensitivity of the AgCl water oxidation system extends from the near UV into the visible light region due to the formation of silver species during the course of the photoreaction, in a process we call self-sensitization. Concisely, the overall reaction can be seen as the oxidation of water to O_2 plus protons and the reduction of silver cations to silver upon illumination. The light absorption can be considered to drive the charge transfer from Cl^- to Ag^+ [eqn. (1)]. The chloride radicals recombine very fast to form Cl_2 [eqn. (2)]. Under suitable conditions ($[Ag^+] \approx 10^{-3}$ M, pH ≈ 4.5) Cl_2 reacts very fast with water to produce hypochlorous acid HOCl [eqn. (3)],

which further decomposes in an Ag^+ catalyzed reaction to form molecular O_2, H^+, and Cl^- [eqn. (4)]. The reduced silver atoms may react with other silver species to form charged silver clusters. Anodic polarization reoxidizes the produced silver species [eqn. (5)]. The AgCl photoanode is polarized at 0.65 V *vs.* a normal hydrogen electrode (NHE). The chloride ions are bound by Ag^+ ions to form AgCl [eqn. (6)]. These reactions are very fast and it is resonable to assume that they take place at or very near the surface of the electrode. The water oxidation reaction and the reoxidation of the reduced silver species take place simultaneously, making the system catalytic. Our understanding of the reaction mechanism and dynamics,[45,46] as well as the system's energetics[45,48] have been reported.

$$[m\mathrm{AgCl}] \xrightarrow{\text{light}} [(m-1)\mathrm{AgCl},\ \mathrm{Ag^0}] + \mathrm{Cl^\bullet} \quad (1)$$

$$2\mathrm{Cl^\bullet} \rightarrow \mathrm{Cl_2} \quad (2)$$

$$\mathrm{Cl_2} + \mathrm{H_2O} \rightarrow \mathrm{HOCl} + \mathrm{H^+} + \mathrm{Cl^-} \quad (3)$$

$$2\mathrm{HOCl} \xrightarrow{\mathrm{Ag^+}} \mathrm{O_2} + 2\mathrm{H^+} + 2\mathrm{Cl^-} \quad (4)$$

$$[(m-1)\mathrm{AgCl},\ \mathrm{Ag^0}] \xrightarrow{\Delta V_{\text{Polarisation}}} [(m-1)\mathrm{AgCl}] + \mathrm{Ag^+} \quad (5)$$

$$[(m-1)\mathrm{AgCl}] + \mathrm{Ag^+} + \mathrm{Cl^-} \rightarrow [m\mathrm{AgCl}] \quad (6)$$

According to the reaction mechanism, the AgCl layer undergoes a morphological change during the experiment, due to the oxidation of silver species and the formation of new AgCl. The morphology of the AgCl layer was investigated by scanning electron microscopy (SEM). Images of electrodes before and after an experiment are shown in Fig. 2. The nanostructure of the layer before the experiment is quite homogeneous with well-defined particles between 200 and 700 nm in diameter (Fig. 2a). The layer has pores and gaps of different size and shape between the particles. Fig. 2b shows a SEM image of an AgCl layer after experiment. After illumination, the layer is rougher and does not appear very homogeneous with a greater range in particle size from about 200 to 1500 nm, and up to 2000 nm for the big one. The layer also appears to be rather uneven with greater cavities between the particles.

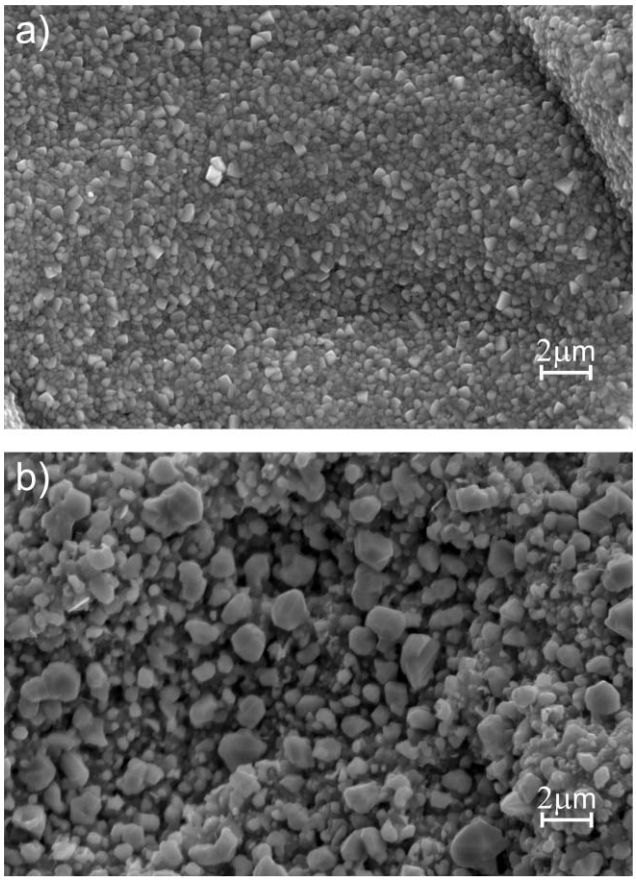

Fig. 2 SEM images of AgCl electrodes, (a) before, (b) after experiment (5000× magnification).

Photoelectrochemical water splitting

The water oxidation experiments led us to water splitting capability tests, as reported in ref. 46. The AgCl system was combined with photocathodic materials like platinized p-$GaInP_2$ and a platinized polycrystalline silicon solar cell. With both types of photocathodes, sustained O_2 and H_2 production was observed. The experiments with p-$GaInP_2$ can be considered as an example where two semiconductor–liquid junctions are used for the photoelectrolysis of water. The results with a platinized polycrystalline silicon solar cell led to a combination of an oxidation photocatalyst with a photovoltaic device. In both systems, the generated potential under illumination was not sufficient to drive the water splitting reaction. For both photocathodic materials, the conduction band position was at a sufficiently negative potential to reduce water to H_2. But the valence band edge was not quite positive enough for driving the oxidation of the silver species in the AgCl system. Therefore, a supplementary external bias by means of a potentiostat had to be applied making the overall water splitting light-assisted.

As amorphous silicon has a higher band gap than polycrystalline silicon, amorphous silicon solar cells were employed in experiments to find out if the AgCl system could work without an additional external bias. The a-Si:H solar cells used were characterized by current–voltage measurements. The light source was the same as for the photoelectrochemical water splitting experiments described below, with an incident intensity of about 100 mW cm^{-2}. Linear potential sweeps were performed with a computer-controlled potentiostat (EG&G, model 273A) where the current was monitored as a function of the applied potential. The front contact of the a-Si:H cell was connected to the working electrode plug. The back contact of the solar cell was used for the counter as well as for the reference electrode plug. The n–i–p a-Si:H solar cells used had an open-circuit voltage around 0.84 V, a short-circuit current density around 9.2 mA cm^{-2}, and a fill factor of 0.5, resulting in an efficiency of the cell of 3.9%. The band gap of the amorphous silicon was approximately 1.8 eV. For details on the preparation and the properties of amorphous silicon solar cells used in this work as well as on n–i–p a-Si:H solar cells with higher efficiency up to 7% (see ref. 43).

An AgCl photoanode was combined with an amorphous silicon solar cell and platinum as cathode. The AgCl layer was employed in the anodic part of a setup for photoelectrochemical water splitting consisting of two separate compartments connected through a salt bridge. A platinum electrode and an amorphous silicon solar cell were used in the cathodic part. In Fig. 3 the O_2 and H_2 production and the anodic photocurrent *vs.* time are shown for several light and dark cycles. Illumination of the AgCl photoanode and the a-Si:H solar cell led to photoelectrochemical water splitting to O_2 and H_2. Sustained and stable O_2 and H_2 production could be observed. The system was exposed to successive illumination and dark periods of 120 and 45 min duration each. The AgCl photoanode showed an O_2 production between 90–100 nmol h^{-1} and the platinum cathode an average H_2 production around 180 nmol h^{-1}. The anodic photocurrent was between 10–11 μA. During the dark periods of an experiment, the O_2 and H_2 sensor signals decreased because of constant inert gas purging.

System energetics

Fig. 4 shows a schematic representation of the principle of the experiment. The approximate position of the band edges for

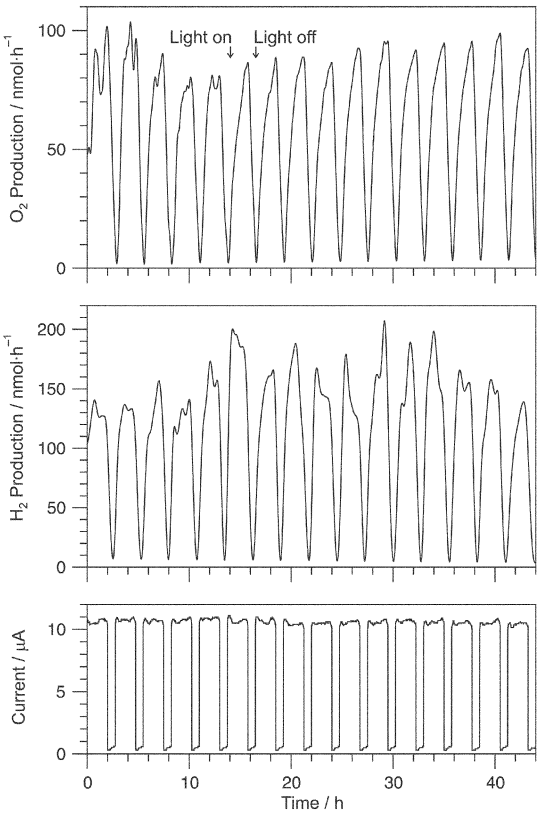

Fig. 3 O_2 and H_2 production and anodic photocurrent *vs.* time for an AgCl layer combined with a Pt cathode and an a-Si:H solar cell for several light and dark cycles.

the a-Si:H solar cell and the AgCl photoanode, the potential range for the silver species, as well as the relevant oxidation and reduction reaction are included. The following considerations were used to draw the scheme.

Fig. 4 has an absolute energy scale on the right and a relative electrochemical potential scale on the left. The electrochemical potential of a redox system is commonly given with respect to a reference electrode, usually the normal hydrogen electrode (NHE).[49] To be able to convert from the electrochemical potential scale in V to the vacuum level energy scale in eV the position of the NHE on the energy scale has to be determined. Usually, a value of −4.5 eV equivalent to 0.0 V *vs.* NHE is used.[50]

For the electron affinity of amorphous silicon the values found in the literature range from 3.7 to 4.0 eV.[51] Assuming an average value of 3.9 eV the position of the conduction band edge can be set at −3.9 eV on the absolute potential energy scale, corresponding to −0.6 V *vs.* NHE. With a band gap energy around 1.8 eV,[43] the position of the valence band edge for amorphous silicon is approximately at −5.7 eV, or at 1.2 V *vs.* NHE. These values were used to set the position of the band edges for the a-Si:H solar cell.

In the absence of silver clusters, AgCl does not absorb light below the indirect band gap transition, which is in the near UV at ≈3.3 eV (≈380 nm).[47,52] The energy of the conduction band edges of AgCl and AgBr are nearly equal, namely at about −3.5 eV.[53] This corresponds to an electrochemical potential of −1.0 V *vs.* NHE. Adding the value of the band gap energy of AgCl we obtain −6.8 eV for the position of the valence band edge, equivalent to 2.3 V on the electrochemical potential scale *vs.* NHE.

The comparison of experimental and calculated values of the ionization energy for differently sized Ag clusters shows that Ag levels are located below the conduction band edge of AgCl. Additional AgCl surface states (SURS), as well as metal induced gap states (MIGS) from Ag/AgCl cluster composites are also present in the band gap region of silver chloride.[45,48] The electrolyte in the photoanode cell is 1 mM in Ag^+, thus, the equilibrium reduction potential for Ag^+ to bulk silver Ag^+/Ag^0_{bulk} is 0.623 V *vs.* NHE ($E°$ for Ag^+/Ag^0_{bulk} is 0.7996 V *vs.* NHE).[49] The reduction potential for silver clusters Ag_n becomes more negative with decreasing cluster size n.[54] Therefore, the value of 0.623 V *vs.* NHE can be considered to be the lower edge of the silver cluster

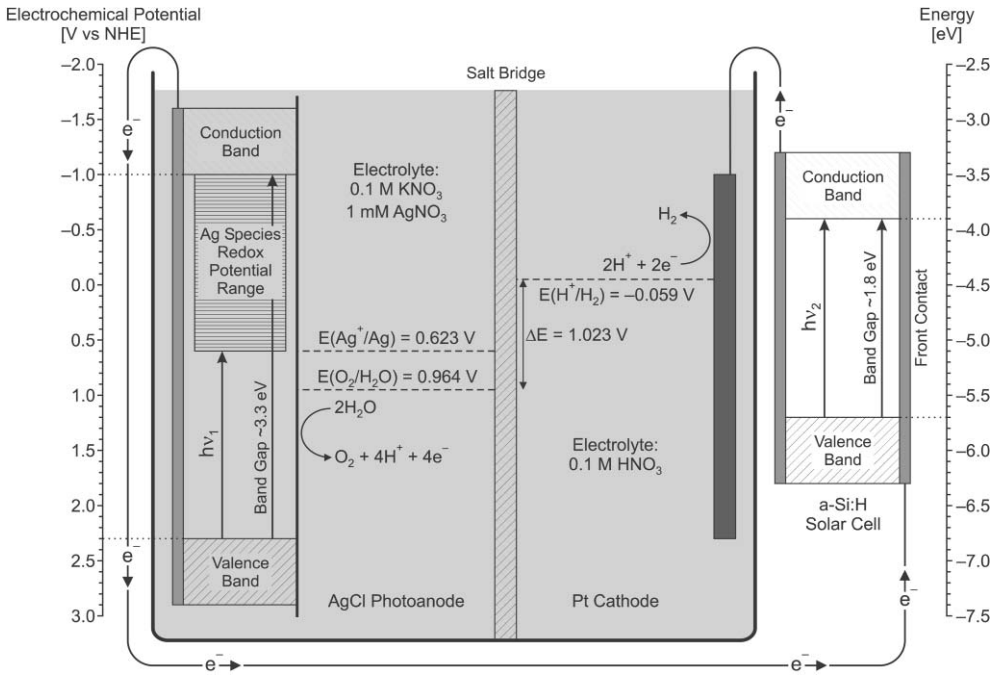

Fig. 4 Schematic representation of the experimental setup with an absolute energy scale on the right and a relative electrochemical potential scale on the left. The AgCl layer was employed in the anodic part of a setup for photoelectrochemical water splitting consisting of two separate compartments connected through a salt bridge. A platinum electrode and an amorphous silicon solar cell were used in the cathodic part. The AgCl photoanode and the platinum cathode are in direct electrolyte contact. The AgCl photoanode and the a-Si:H solar cell were simultaneously illuminated. The electrochemical potential of the pH dependent redox reactions is given according to the pH inside the cell compartment (pH ≈ 4.5 for the photoanode cell, pH ≈ 1.0 for the cathode cell). Consequently, the chemical bias due to the pH gradient between the compartments is 0.21 V. For a different chemical bias the potential of pH dependent redox reactions has to be shifted accordingly.

redox potential range. All these different levels are responsible for the self-sensitization of AgCl. They extend ≈1.6 eV below the conduction band of silver chloride. Electron transitions from the AgCl valence band to empty levels below the conduction band are possible. Nevertheless, these new optical transitions in the visible spectral range can still initiate the oxidation of water, because the conduction band is not directly involved in the oxidation process. Thus, the photocatalytic oxidation of water with AgCl is extended from the near UV into the visible part of the spectrum. This interpretation is consistent with the response and the onset of the contact potential difference signal from surface photovoltage spectroscopy (SPS) measurements carried out with AgCl layers.[46]

In the following discussion of the water oxidation and reduction reaction we assume a purely thermodynamic system. We neglect that for a dynamic system reaction kinetics plays a central role and among other requirements, a significant overpotential is needed for actually splitting water at an appreciable rate. For the water splitting reaction, $2H_2O \rightarrow 2H_2 + O_2$, 1.229 V must be provided for the reaction to proceed at standard conditions.[49] In our experimental setup the oxidation and reduction process are carried out in two separate compartments. The overall water splitting reaction is pH independent, but the oxidation and reduction reaction depend on pH. The thermodynamic potential varies by ±0.059 V for every pH unit difference between the anode and cathode compartment. A pH gradient between the compartments can be regarded as chemical bias. The pH in the photoanode cell was maintained at ≈4.5. Assuming that the relevant redox couple is O_2/H_2O, the potential for the oxidation half-cell reaction at a pH of 4.5 is 0.964 V. The redox couple in the cathode compartment is H^+/H_2, leading to a potential of −0.059 V at pH ≈ 1.0 for the reduction half-cell reaction. Consequently, the chemical bias due to the pH gradient between the compartments is 0.21 V. This means that a potential of 1.023 V has at least to be supplied by our system, *i.e.* the AgCl photoanode and the a-Si:H solar cell, to drive the overall water splitting reaction under illumination.

The AgCl photoanode was responsible for the oxidation of water to O_2, whereas on the cathode water was reduced to H_2. The AgCl photoanode and the platinum cathode were in direct electrolyte contact. An amorphous silicon solar cell was used for the electron transfer from the photoanode to the cathode. The conduction band edge of the a-Si:H solar cell is at a more negative electrochemical potential with respect to the redox couple H^+/H_2 and the valence band edge of the AgCl photoanode is at a more positive potential with respect to the O_2/H_2O redox couple. This means, that photogenerated conduction band electrons from the a-Si:H solar cell can reduce H^+ to H_2, while the photogenerated holes in the valence band of AgCl do initiate the oxidation of water to O_2.

The sensitivity of the AgCl water oxidation system extends from the near UV into the visible light region due to the formation of silver species during the course of the photoreaction (self-sensitization). The silver species have to be reoxidized to make the system catalytic. A comparison with our previous results where a platinized polycrystalline silicon solar cell was used as photovoltaic device shows, that the position of the valence band in the photovoltaic part is important for the oxidation of the silver species.[46] The valence band edge of crystalline silicon is not at a sufficiently positive potential for driving the oxidation of the silver species in the AgCl system. Therefore, a supplementary external bias by means of a potentiostat had to be applied for these experiments, making the overall water splitting light-assisted. However, the valence band edge of amorphous silicon has a lower energy than the edge of the silver species redox potential range. The potential required for the reoxidation of the silver species on the AgCl photoanode is entirely supplied by the a-Si:H solar cell. The electron transfer from the photoanode cell to the cathode cell is only achieved by illumination. No additional external bias has to be applied.

AgCl layers modified with Au colloids

We have also carried out water oxidation experiments with AgCl layers in a flow photoreactor system, where anodic polarization of the AgCl electrode by means of a potentiostat was used for reoxidizing the produced silver species. They showed that AgCl layers modified with Au colloids have a higher photoactivity compared to AgCl layers without Au colloids. The O_2 production and the photocurrent were increased by a factor of about three. Details on the effect of gold colloids on the photocatalytic oxidation of water to O_2 with silver chloride as photocatalyst were reported elsewhere.[44] Therefore, a number of photoelectrochemical water splitting experiments were also carried out with gold colloid modified AgCl layers. Gold colloids were produced by reduction of gold chloride with sodium citrate. This method was found to be particularly easy and suitable for our studies in aqueous solution. The colloids produced are spherical in shape with a diameter of 15–20 nm (see Experimental).[42] The gold particles were sedimented on the AgCl layer by immersing it overnight into a colloidal solution. In Fig. 5 the O_2 and H_2 production and the anodic photocurrent *vs.* time for an AgCl layer modified with Au colloids are shown for several light and dark cycles. The AgCl photoanode showed an O_2 production around 190 nmol h^{-1} and the platinum cathode an average H_2 production around 380 nmol h^{-1}. The anodic photocurrent was around 22 μA. Averaging over several experiments, we observed that small traces of Au colloids greatly influenced the photoelectrochemical activity of the AgCl system. The O_2 and H_2 production, as well as the photocurrent were usually increased by a factor of 1.5–2, depending on the layer's performance. Taking into account the differences in the experimental setups and conditions, this improvement can be considered satisfactory compared to the increase in O_2 production and photocurrent for experiments carried out in a flow photoreactor mentioned above.

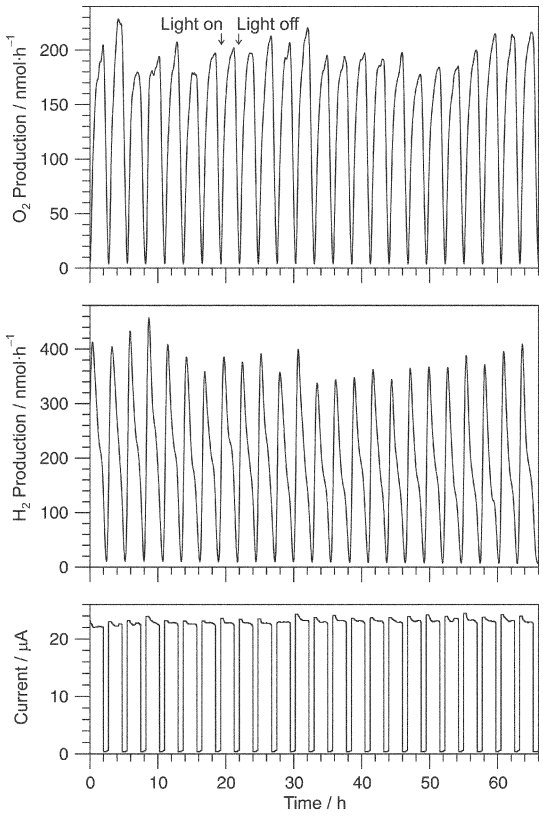

Fig. 5 O_2 and H_2 production and anodic photocurrent *vs.* time for an AgCl layer modified with Au colloids combined with a Pt cathode and an a-Si:H solar cell for several light and dark cycles.

In situ characterization of AgCl electrodes were carried out with UV/vis diffuse reflectance spectroscopy. Silver chloride layers modified with gold colloids show throughout the experiment a higher absorbance of about 20% compared to layers without colloids.[44] The higher absorbance cannot account for the increased activity of gold modified AgCl layers. It has been reported that gold deposited on TiO_2 nanoparticles promotes the charge transfer process at the semiconductor/electrolyte interface, improving the photocatalytic oxidation capability of the semiconductor.[55] Deposition of Au particles on Fe_2O_3 film also increased the anodic photocurrent by promoting the transfer of holes in the conduction band of the semiconductor to the electrolyte.[56] The hole transfer in the oxidation process is improved because the metal nanoparticles on the semiconductor accept greater amounts of electrons.[57] A similar effect has also to be considered in the present case. Therefore, the higher photoactivity of gold modified AgCl layers can be explained by an increased absorption of the layer due to Au colloids (spectral sensitization), as well as the effect of gold particles in promoting the charge transfer process at the semiconductor/electrolyte interface, improving the photocatalytic oxidation capability of the AgCl system.

To support the discussion on the energetics of the system another experiment with an AgCl layer modified with Au colloids was carried out. In Fig. 6 the O_2 and H_2 production and the anodic photocurrent *vs.* time are shown for several light and dark cycles. For the first two cycles the AgCl photoanode as well as the a-Si:H solar cell were illuminated. The AgCl layer showed an O_2 production around 140 nmol h^{-1} and the platinum cathode an average H_2 production around 280 nmol h^{-1}. The anodic photocurrent was around 17 μA. For cycle 3 only the AgCl photoanode was illuminated. No photocurrent, and consequently no H_2 production is observed because the a-Si:H solar cell was not illuminated. On the other hand, the amount of O_2 produced is comparable with the previous cycles, showing that the water oxidation capability does not depend on the solar cell being illuminated.

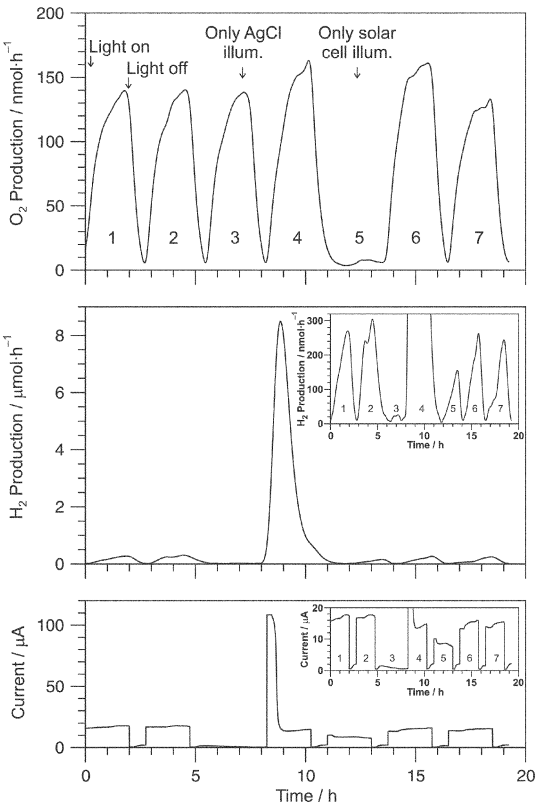

Fig. 6 O_2 and H_2 production and anodic photocurrent *vs.* time for an AgCl layer modified with Au colloids combined with a Pt cathode and an a-Si:H solar cell. Cycles 1, 2, 4, 6, and 7: AgCl photoanode and a-Si:H solar cell were illuminated. Cycle 3: only AgCl layer was illuminated. Cycle 5: only a-Si:H solar cell was illuminated. The insets show the same graph with a different scale.

For cycle 4, both the AgCl photoanode and the a-Si:H solar cell were illuminated again. For the H_2 signal and the photocurrent a high increase is observed. The H_2 production rate rises up to 8 μmol h^{-1} and the photocurrent peaks at 110 μA. The increase is due to accumulated Ag species from the previous cycle, which were not reoxidized because the a-Si:H solar cell was not illuminated. In the second part of the cycle, both signals start to decrease, though the H_2 signal is delayed due to a slower response of the sensor. As expected, the corresponding O_2 signal is not affected, having a comparable rate to the proceeding cycles.

For cycle 5 only the a-Si:H solar cell was illuminated. The lower H_2 production around 150 nmol h^{-1} and the photocurrent around 8 μA are due to Ag species present on the layer which were not reoxidized in the previous cycle. No O_2 is produced when the AgCl layer is not illuminated. Hence, the amorphous silicon solar cell is only responsible for the electron transfer from the anodic to the cathodic part of the setup by reoxidizing the produced silver species, as well as for the hydrogen production on the platinum cathode. For the last two cycles, 6 and 7, the AgCl photoanode as well as the a-Si:H solar cell were illuminated again. The O_2 and H_2 production as well as the photocurrent reach comparable values like in cycle 1 and 2. Concisely, the results shown in Fig. 6 are in agreement with the mechanism and the discussion on the system's energetics above.

Conclusions

For the first time, AgCl photoanodes were used for the photoelectrolysis of water without applying a polarization potential by means of a potentiostat. An AgCl photoanode was combined with a platinum cathode and an amorphous silicon solar cell. The O_2 producing AgCl system was coupled to a platinum cathode and a photovoltaic device, leading to an overall water splitting system. Amorphous silicon has a suitable position of the conduction band for the H_2 production, as well as a valence band position, due to a sufficiently large band gap, capable to drive the oxidation of the reduced silver species in the AgCl system. Although a small chemical bias due to the pH gradient between the anode and cathode compartment is present, AgCl photoanodes combined with a-Si:H solar cells and platinum as cathode showed the ability of the system to split water.

An increased photocurrent, and consequently a higher O_2 and H_2 production were observed with AgCl electrodes modified with Au colloids. Small traces of Au colloids greatly influenced the photoelectrochemical activity of the AgCl system. The O_2 and H_2 production, as well as the photocurrent were increased by a factor of 1.5–2, depending on the layer's performance. The higher photoactivity of gold modified AgCl layers can be explained by an increased absorption of the layer due to Au colloids (spectral sensitization), as well as the effect of gold particles in promoting the charge transfer process at the semiconductor/electrolyte interface, improving the photocatalytic oxidation capability of the AgCl system.

As mentioned in the introduction, in other reports multiple junction amorphous silicon solar cells were used in a photovoltaic system for the photoelectrolysis of water. In our arrangement a basic single junction a-Si:H solar cell with a relatively low efficiency of 3.9% was employed. When combined with an AgCl photoanode, the a-Si:H solar cell was sufficient to form a photovoltaic/semiconductor system, though our reported photocurrent and O_2 and H_2 production is low compared to the multiple junction approach.

The overall efficiency of the system is still low. Much improvement is required especially in the photocatalytic activity of the AgCl photoanode, which we intend to achieve by further modifying the preparation and sensitization process of the layer. A higher efficiency is also important for the system to work in

the absence of a chemical bias. Successful tests have already been carried out, though at the present stage with a lower current density, and consequently a lower O_2 and H_2 production, showing the importance of further reducing the overpotential barrier at both the photoanode and the photocathode.

The presented results are very encouraging. In a next step, amorphous silicon solar cells could be integrated inside the cathode compartment of the experimental setup and used as photocathode for the H_2 production. In this case, the front surface of the cell has to be protected and the back surface of the stainless steel support should be able to produce H_2, for example by modifying it with a reduction catalyst like platinum.

Acknowledgements

This work was supported by the Swiss Federal Office of Energy (project no. 36846) and the Swiss National Science Foundation (project no. 2000-067684). We thank Adrian Schindler for the PVD coating of the glass supports, Beatrice Frey and Beatrice Koppel for the SEM images, and Karine van der Werf for depositing the amorphous silicon solar cells. We also thank Professor Gary Hodes (Weizmann Institute of Science, Rehovot, Israel) for helpful discussions.

References

1 *United Nations Framework Convention on Climate Change (UNFCCC)*, Kyoto Protocol, Bonn, Germany, 1997, www.unfccc.int.

2 A. Meyer, *Contraction and Convergence - The Global Solution to Climate Change*, Green Books Ltd, UK, 2000; A. Meyer, Global Commons Institute (GCI), www.gci.org.uk.

3 (*a*) J. A. Turner, A Realizable Renewable Energy Future, *Science*, 1999, **285**, 687–689; (*b*) C. C. Elam, C. E. G. Padró, G. Sandrock, A. Luzzi, P. Lindblad and E. F. Hagen, Realizing the hydrogen future: the International Energy Agency's efforts to advance hydrogen energy technologies, *Int. J. Hydrogen Energy*, 2003, **28**, 601–607.

4 (*a*) A. Zouni, H. T. Witt, J. Kern, P. Fromme, N. Krauss, W. Saenger and P. Orth, Crystal structure of photosystem II from Synechococcus elongatus at 3.8 Å resolution, *Nature*, 2001, **409**, 739–743; (*b*) F. Mamedov and S. Styring, Logistics in the life cycle of Photosystem II–lateral movement in the thylakoid membrane and activation of electron transfer, *Physiol. Plant.*, 2003, **119**, 328–336; (*c*) R. Harrer, Aus Licht wird Leben–Proteine der Photosynthese, *Chem. Unserer Zeit*, 2003, **37**, 234–241 and references therein.

5 J. R. Bolton, Solar photoproduction of Hydrogen: A review, *Solar Energy*, 1996, **57**, 37–50.

6 T. Bak, J. Nowotny, M. Rekas and C. C. Sorrell, Photoelectrochemical hydrogen generation from water using solar energy. Materials-related aspects, *Int. J. Hydrogen Energy*, 2002, **27**, 991–1022.

7 A. J. Nozik, Photochemical diodes, *Appl. Phys. Lett.*, 1977, **30**, 567–569.

8 S. Licht, Multiple Band Gap Semiconductor/Electrolyte Solar Energy Conversion, *J. Phys. Chem. B*, 2001, **105**, 6281–6294.

9 (*a*) S. S. Kocha, D. Montgomery, M. W. Peterson and J. A. Turner, Photoelectrochemical decomposition of water utilizing monolithic tandem cells, *Sol. Energy Mater. Sol. Cells*, 1998, **52**, 389–397; (*b*) O. Khaselev and J. A. Turner, A Monolithic Photovoltaic-Photoelectrochemical Device for Hydrogen Production *via* Water Splitting, *Science*, 1998, **280**, 425–427; (*c*) X. Gao, S. Kocha, A. J. Frank and J. A. Turner, Photoelectrochemical decomposition of water using modified monolithic tandem cells, *Int. J. Hydrogen Energy*, 1999, **24**, 319–325.

10 O. Khaselev, A. Bansal and J. A. Turner, High-efficiency integrated multijunction photovoltaic/electrolysis systems for hydrogen production, *Int. J. Hydrogen Energy*, 2001, **26**, 127–132.

11 (*a*) S. Licht, B. Wang, S. Mukerji, T. Soga, M. Umeno and H. Tributsch, Efficient Solar Water Splitting Exemplified by RuO_2-Catalyzed AlGaAs/Si Photoelectrolysis, *J. Phys. Chem. B*, 2000, **104**, 8920–8924; (*b*) S. Licht, B. Wang, S. Mukerji, T. Soga, M. Umeno and H. Tributsch, Over 18% solar energy conversion to generation of hydrogen fuel: theory and experiment for efficient solar water splitting, *Int. J. Hydrogen Energy*, 2001, **26**, 653–659.

12 E. L. Miller, R. E. Rocheleau and X. M. Deng, Design considerations for a hybrid amorphous silicon/photoelectrochemical multijunction cell for hydrogen production, *Int. J. Hydrogen Energy*, 2003, **28**, 615–623.

13 (*a*) S. Licht, Solar Water Splitting To Generate Hydrogen Fuel: Photothermal Electrochemical Analysis, *J. Phys. Chem. B*, 2003, **107**, 4253–4260; (*b*) S. Licht, L. Halperin, M. Kalina, M. Zidman and N. Halperin, Electrochemical potential tuned solar water splitting, *Chem. Commun.*, 2003, 3006–3007.

14 Z. Zou, J. Ye and H. Arakawa, Photocatalytic water splitting into H_2 and/or O_2 under UV and visible light irradiation with a semiconductor photocatalyst, *Int. J. Hydrogen Energy*, 2003, **28**, 663–669.

15 (*a*) Z. Zou, J. Ye, K. Sayama and H. Arakawa, Direct splitting of water under visible light irradiation with an oxide semiconductor photocatalyst, *Nature*, 2001, **414**, 625–627; (*b*) Z. Zou and H. Arakawa, Direct water splitting into H_2 and O_2 under visible light irradiation with a new series of mixed oxide semiconductor photocatalysts, *J. Photochem. Photobiol. A: Chem.*, 2003, **158**, 145–162.

16 (*a*) H. G. Kim, D. W. Hwang, S. W. Bae, J. H. Jung and J. S. Lee, Photocatalytic water splitting over $La_2Ti_2O_7$ synthesized by the polymerizable complex method, *Catal. Lett.*, 2003, **91**, 193–198; (*b*) D. W. Hwang, J. S. Lee, W. Li and S. H. Oh, Electronic Band Structure and Photocatalytic Activity of $Ln_2Ti_2O_7$ (Ln = La, Pr, Nd), *J. Phys. Chem. B*, 2003, **107**, 4963–4970.

17 J. Yin, Z. Zou and J. Ye, A Novel Series of the New Visible-Light-Driven Photocatalysts $MCo_{1/3}Nb_{2/3}O_3$ (M = Ca, Sr, and Ba) with Special Electronic Structures, *J. Phys. Chem. B*, 2003, **107**, 4936–4941.

18 (*a*) M. Machida, J. Yabunaka and T. Kijima, Synthesis and Photocatalytic Property of Layered Perovskite Tantalates, $RbLnTa_2O_7$ (Ln = La, Pr, Nd, and Sm), *Chem. Mater.*, 2000, **12**, 812–817; (*b*) M. Machida, K. Miyazaki, S. Matsushima and M. Arai, Photocatalytic properties of layered perovskite tantalates, $MLnTa_2O_7$ (M = Cs, Rb, Na, and H; Ln = La, Pr, Nd, and Sm), *J. Mater. Chem.*, 2003, **13**, 1433–1437.

19 (*a*) H. Kato, K. Asakura and A. Kudo, Highly Efficient Water Splitting into H_2 and O_2 over Lanthanum-Doped $NaTaO_3$ Photocatalysts with High Crystallinity and Surface Nanostructure, *J. Am. Chem. Soc.*, 2003, **125**, 3082–3089; (*b*) A. Yamakata, T. Ishibashi, H. Kato, A. Kudo and H. Onishi, Photodynamics of $NaTaO_3$ Catalysts for Efficient Water Splitting, *J. Phys. Chem. B*, 2003, **107**, 14383–14387; (*c*) H. Kato and A. Kudo, Photocatalytic water splitting into H_2 and O_2 over various tantalate photocatalysts, *Catal. Today*, 2003, **78**, 561–569.

20 R. Abe, M. Higashi, Z. Zou, K. Sayama, Y. Abe and H. Arakawa, Photocatalytic Water Splitting into H_2 and O_2 over R_3TaO_7 and R_3NbO_7 (R = Y, Yb, Gd, La): Effect of Crystal Structure on Photocatalytic Activity, *J. Phys. Chem. B*, 2004, **108**, 811–814.

21 M. D. Archer and J. R. Bolton, Requirements for Ideal Performance of Photochemical and Photovoltaic Solar Energy Converters, *J. Phys. Chem.*, 1990, **94**, 8028–8036.

22 T. Inoue and T. Yamase, Photoelectrochemical cell using SiC for water splitting, *Chem. Lett.*, 1985, 869–872.

23 K. Sayama, K. Mukasa, R. Abe, Y. Abe and H. Arakawa, A new photocatalytic water splitting system under visible light irradiation mimicking a Z-scheme mechanism in photosynthesis, *J. Photochem. Photobiol. A: Chem.*, 2002, **148**, 71–77.

24 H. Mettee, J. W. Otvos and M. Calvin, Solar induced water splitting with p/n heterotype photochemical diodes: n-Fe_2O_3/p-GaP, *Sol. Energy Mater.*, 1981, **4**, 443–453.

25 V. M. Aroutiounian, V. M. Arakelyan, G. E. Shahnazaryan, G. M. Stepanyan, J. A. Turner and O. Khaselev, Investigation of ceramic Fe_2O_3<Ta> photoelectrodes for solar energy photoelectrochemical converters, *Int. J. Hydrogen Energy*, 2002, **27**, 33–38.

26 Y. Bessekhouad, M. Trari and J. P. Doumerc, $CuMnO_2$ - a novel hydrogen photoevolution catalyst, *Int. J. Hydrogen Engery*, 2003, **28**, 43–48.

27 (*a*) M. Matsumura, Y. Saho and H. Tsubomura, Photocatalytic Hydrogen Production from Solutions of Sulfite Using Platinized Cadmium Sulfide Powder, *J. Phys. Chem.*, 1983, **87**, 3807–3808; (*b*) J. F. Reber and M. Rusek, Photochemical Hydrogen Production with Platinized Suspensions of Cadmium Sulfide and Cadmium Zinc Sulfide Modified by Silver Sulfide, *J. Phys. Chem.*, 1986, **90**, 824–834; (*c*) M. Subrahmanyam, V. T. Supiya and P. R. Reddy, Photocatalytic H_2 production with CdS-based catalysts from a sulfide/sulfite substrate: An effort to develop MgO-supported catalysts, *Int. J. Hydrogen Energy*, 1996, **21**, 99–106.

28 T. Kida, G. Guan, Y. Minami, T. Ma and A. Yoshida, Photocatalytic hydrogen production from water over a $LaMnO_3$/CdS nanocomposite prepared by the reverse micelle method, *J. Mater. Chem.*, 2003, **13**, 1186–1191.

29 (*a*) A. Sobczynski, A. Yildiz, A. J. Bard, A. Campion, M. A. Fox, T. Mallouk, S. E. Webber and J. M. White, Tungsten Disulfide: A Novel Hydrogen Evolution Catalyst for Water Decomposition, *J. Phys. Chem.*, 1988, **92**, 2311–2315; (*b*) K. Gurunathan, N. Velmani

and P. Maruthamuthu, Photocatalytic hydrogen production using dye-sensitized metal ions dipoled WS2 semiconductor powders in presence of electron relay, *Bull. Electrochem.*, 1996, **12**, 387–390.
30 A. Ishikawa, T. Takata, T. Matsumura, J. N. Kondo, M. Hara, H. Kobayashi and K. Domen, Oxysulfides $Ln_2Ti_2S_2O_5$ as Stable Photocatalysts for Water Oxidation and Reduction under Visible-Light Irradiation, *J. Phys. Chem. B*, 2004, **108**, 2637–2642.
31 J. Yin, Z. Zou and J. Ye, Photophysical and photocatalytic properties of new photocatalysts $MCrO_4$ (M = Sr, Ba), *Chem. Phys. Lett.*, 2003, **378**, 24–28.
32 (*a*) W. Rüttinger and G. D. Dismukes, Synthetic Water-Oxidation Catalysts for Artificial Photosynthetic Water Oxidation, *Chem. Rev.*, 1997, **97**, 1–24; (*b*) *Biochim. Biophys. Acta Bioenerg.*, 2001, **1503**(special issue), 1–259.
33 (*a*) W. Rüttinger, M. Yagi, K. Wolf, S. Bernasek and G. C. Dismukes, O_2 Evolution from the Manganese-Oxo Cubane Core $Mn_4O_4^{6+}$: A Molecular Mimic of the Photosynthetic Water Oxidation Enzyme?, *J. Am. Chem. Soc.*, 2000, **122**, 10353–10357; (*b*) J. Limburg, J. S. Vrettos, H. Chen, J. C. de Paula, R. H. Crabtree and G. W. Brudvig, Characterization of the O_2-Evolving Reaction Catalyzed by $[(terpy)(H_2O)Mn^{III}(O)_2Mn^{IV}(OH_2)(terpy)](NO_3)_3$ (terpy = 2,2′:6,2″-terpyridine), *J. Am. Chem. Soc.*, 2001, **123**, 423–430; (*c*) M. Yagi and M. Kaneko, Molecular Catalysts for Water Oxidation, *Chem. Rev.*, 2001, **101**, 21–35; (*d*) M. Yagi, K. V. Wolf, P. J. Baesjou, S. L. Bernasek and G. C. Dismukes, Selective Photoproduction of O_2 from the Mn_4O_4 Cubane Core: A Structural and Functional Model for the Photosynthetic Water-Oxidizing Complex, *Angew. Chem.*, 2001, **113**, 3009–3012; (*e*) M. Yagi, K. V. Wolf, P. J. Baesjou, S. L. Bernasek and G. C. Dismukes, *Angew. Chem., Int. Ed.*, 2001, **40**, 2925–2928; (*f*) Y. Shimazaki, T. Nagano, H. Takesue, B. H. Ye, F. Tani and Y. Naruta, Characterization of a Dinuclear Mn^{V}=O Complex and Its Efficient Evolution of O_2 in the Presence of Water, *Angew. Chem.*, 2004, **116**, 100–102; (*g*) Y. Shimazaki, T. Nagano, H. Takesue, B. H. Ye, F. Tani and Y. Naruta, *Angew. Chem., Int. Ed.*, 2004, **43**, 98–100.
34 H. Shiroishi, M. Nukaga, S. Yamashita and M. Kaneko, Efficient Photochemical Water Oxidation by a Molecular Catalyst Immobilized onto Metal Oxides, *Chem. Lett.*, 2002, 488–489.
35 (*a*) A. Fujishima, K. Kohayakawa and K. Honda, Hydrogen Production under Sunlight with an Electrochemical Photocell, *J. Electrochem. Soc.*, 1975, **122**, 1487–1489; (*b*) S. U. M. Khan, M. Al-Shahry and W. B. Ingler, Jr, Efficient Photochemical Water Splitting by a Chemically Modified n-TiO_2, *Science*, 2002, **297**, 2243–2245.
36 G. R. Torres, T. Lindgren, J. Lu, C. G. Granqvist and S. E. Lindquist, Photoelectrochemical Study of Nitrogen-Doped Titanium Dioxide for Water Oxidation, *J. Phys. Chem. B*, 2004, **108**, 5995–6003.
37 (*a*) K. Sayama, R. Yoshida, H. Kusama, K. Okabe, Y. Abe and H. Arakawa, Photocatalytic decomposition of water into H_2 and O_2 by a two-step photoexcitation reaction using a WO_3 suspension catalyst and an Fe^{3+}/Fe^{2+} redox system, *Chem. Phys. Lett.*, 1997, **277**, 387–391; (*b*) H. Wang, T. Lindgren, J. He, A. Hagfeldt and S. E. Lindquist, Photoelectrochemistry of Nanostructured WO_3 Thin Film Electrodes for Water Oxidation: Mechanism of Electron Transport, *J. Phys. Chem. B*, 2000, **104**, 5686–5696; (*c*) C. Santato, M. Ulmann and J. Augustynski, Photoelectrochemical Properties of Nanostructured Tungsten Trioxide Films, *J. Phys. Chem. B*, 2001, **105**, 936–940; (*d*) C. Santato, M. Odziemkowski, M. Ulmann and J. Augustynski, Crystallographically Oriented Mesoporous WO_3 Films: Synthesis, Characterization, and Applications, *J. Am. Chem. Soc.*, 2001, **123**, 10639–10649.
38 D. W. Hwang, J. Kim, T. J. Park and J. S. Lee, Mg-doped WO_3 as a novel photocatalyst for visible light-induced water splitting, *Catal. Lett.*, 2002, **80**, 53–57.
39 (*a*) S. U. M. Khan and J. Akikusa, Photoelectrochemical Splitting of Water at Nanocrystalline n-Fe_2O_3 Thin-Film Electrodes, *J. Phys. Chem. B*, 1999, **103**, 7184–7189; (*b*) C. J. Sartoretti, M. Ulmann, B. D. Alexander, J. Augustynski and A. Weidenkaff, Photoelectrochemical oxidation of water at transparent ferric oxide film electrodes, *Chem. Phys. Lett.*, 2003, **376**, 194–200.
40 K. Sayama, A. Nomura, Z. Zou, R. Abe, Y. Abe and H. Arakawa, Photoelectrochemical decomposition of water on nanocrystalline $BiVO_4$ film electrodes under visible light, *Chem. Commun.*, 2003, 2908–2909.
41 (*a*) M. Grätzel and R. K. Thampi, Patent Application, European Patent Office, EP 1 175 938 A1; (*b*) M. Grätzel and J. Augustynski, Patent Application, World Intellectual Property Organization, WO 01/02624 A1; (*c*) M. Grätzel, The artificial leaf, bio-mimetic photocatalysis, *Cattech*, 1999, **3**, 4–16.
42 (*a*) J. Turkevich, P. C. Stevenson and J. Hillier, A study of the nucleation and growth processes in the synthesis of colloidal gold, *Discuss. Faraday Soc.*, 1951, **11**, 55–75; (*b*) J. Turkevich, P. C. Stevenson and J. Hillier, The formation of colloidal gold, *J. Phys. Chem.*, 1953, **57**, 670–673; (*c*) P. C. Lee and D. Meisel, Adsorption and Surface-Enhanced Raman of Dyes on Silver and Gold Sols, *J. Phys. Chem.*, 1982, **86**, 3391–3395.
43 (*a*) M. K. van Veen and R. E. I. Schropp, Beneficial effect of a low deposition temperature of hot-wire deposited intrinsic amorphous silicon for solar cells, *J. Appl. Phys.*, 2003, **93**, 121–125; (*b*) M. K. van Veen and R. E. I. Schropp, Understanding shunting behavior in hot-wire-deposited amorphous silicon solar cells, *Appl. Phys. Lett.*, 2003, **82**, 287–289; (*c*) M. K. van Veen, PhD Thesis, Utrecht University, The Netherlands, 2003.
44 A. Currao, V. R. Reddy and G. Calzaferri, Gold-Colloid-Modified AgCl Photocatalyst for Water Oxidation to O_2, *ChemPhysChem*, 2004, **5**, 720–724.
45 (*a*) K. Pfanner, N. Gfeller and G. Calzaferri, Photochemical oxidation of water with thin AgC1 layers, *J. Photochem. Photobiol. A: Chem.*, 1996, **95**, 175–180; (*b*) M. Lanz, D. Schürch and G. Calzaferri, Photocatalytic oxidation of water to O_2 on AgCl-coated electrodes, *J. Photochem. Photobiol. A: Chem.*, 1999, **120**, 105–117; (*c*) G. Calzaferri, D. Brühwiler, S. Glaus, D. Schürch, A. Currao and C. Leiggener, Quantum-Sized Silver, Silver Chloride and Silver Sulfide Clusters, *J. Imaging Sci. Technol.*, 2001, **45**, 331–339.
46 (*a*) D. Schürch, A. Currao, S. Sarkar, G. Hodes and G. Calzaferri, The Silver Chloride Photoanode in Photoelectrochemical Water Splitting, *J. Phys. Chem. B*, 2002, **106**, 12764–12775; (*b*) D. Schürch and A. Currao, The AgCl Photoanode for Photoelectrochemical Water Splitting, *Chimia*, 2003, **57**, 204–207.
47 S. Glaus and G. Calzaferri, The band structures of the silver halides AgF, AgCl, and AgBr: A comparative study, *Photochem. Photobiol. Sci.*, 2003, **2**, 398–401.
48 (*a*) S. Glaus and G. Calzaferri, Silver Chloride Clusters and Surface States, *J. Phys. Chem. B*, 1999, **103**, 5622–5630; (*b*) S. Glaus, G. Calzaferri and R. Hoffmann, Electronic Properties of the Silver–Silver Chloride Cluster Interface, *Chem. Eur. J.*, 2002, **8**, 1785–1794.
49 *CRC Handbook of Chemistry and Physics*, ed. D. R. Lide and H. P. R. Frederikse, CRC Press, Boca Raton, FL, 78th edn., 1998, p. 8-20-8-30.
50 F. Lohmann, Fermi-Niveau und Flachbandpotential von Molekülkristallen aromatischer Kohlenwasserstoffe, *Z. Naturforsch.*, 1967, **22a**, 843–844.
51 F. Smole, M. Topic and J. Furlan, Analysis of TCO/p(a-Si:C:H) heterojunction and its influence on p–i–n a-Si:H solar cell performance, *J. Non-Cryst. Solids*, 1996, **194**, 312–318.
52 (*a*) Y. Poisant, P. Chatterjee and P. Roca i Cabarrocas, No benefit from microcrystalline silicon N layers in single junction amorphous silicon p–i–n solar cells, *J. Appl. Phys.*, 2003, **93**, 170–174; (*b*) A. P. Marchetti and R. S. Eachus, The photochemistry and photophysics of the silver halides, *Adv. Photochem.*, 1992, **17**, 145–216.
53 (*a*) F. C. Brown, Electronic properties and band structure of the silver halides, *J. Phys. Chem.*, 1962, **66**, 2368–2376; (*b*) S. Sumi, T. Watanabe, A. Fujishima and K. Honda, Effect of Cl^- and Br^- Ions and pH on the Flatband Potentials of Silver Halide Sheet Crystal Electrodes, *Bull. Chem. Soc. Jpn.*, 1980, **53**, 2742–2747; (*c*) M. Kawasaki, H. Hada and H. Uchida, Transfer of photoelectrons and photoholes through a AgBr/AgCl interface and relative locations of the energy bands, *J. Appl. Phys.*, 1986, **60**, 3945–3953.
54 (*a*) W. J. Plieth, Electrochemical Properties of Small Clusters of Metal Atoms and Their Role in Surface Enhanced Raman Scattering, *J. Phys. Chem.*, 1982, **86**, 3166–3170; (*b*) A. Henglein, Remarks on the Electrochemical Potential of Small Silver Clusters in Aqueous Solution, *Ber. Bunsen-Ges. Phys. Chem.*, 1990, **94**, 600–603.
55 (*a*) N. Chandrasekharan and P. V. Kamat, Improving the Photoelectrochemical Performance of Nanostructured TiO_2 Films by Adsorption of Gold Nanoparticles, *J. Phys. Chem. B*, 2000, **104**, 10851–10857; (*b*) A. Dawson and P. V. Kamat, Semiconductor-Metal Nanocomposites. Photoinduced Fusion and Photocatalysis of Gold-Capped TiO_2 (TiO_2/Gold) Nanoparticles, *J. Phys. Chem. B*, 2001, **105**, 960–966; (*c*) V. Subramanian, E. Wolf and P. V. Kamat, Semiconductor-Metal Composite Nanostructures. To What Extent Do Metal Nanoparticles Improve the Photocatalytic Activity of TiO_2 Films?, *J. Phys. Chem. B*, 2001, **105**, 11439–11446.
56 A. Watanabe and H. Kozuka, Photoanodic Properties of Sol-Gel-Derived Fe_2O_3 Thin Films Containing Dispersed Gold and Silver Particles, *J. Phys. Chem. B*, 2003, **107**, 12713–12720.
57 V. Subramanian, E. E. Wolf and P. V. Kamat, Catalysis with TiO_2/Gold Nanocomposites. Effect of Metal Particle Size on the Fermi Level Equilibration, *J. Am. Chem. Soc.*, 2004, **126**, 4943–4950.